Available online at www.sciencedirect.com

ScienceDirect

Scripta Materialia 106 (2015) 46–51

Scripta MATERIALIA

www.elsevier.com/locate/scriptamat

Stagnation accommodated global plasticity in nanoglass composites

Li Yao[a] and Zhao-Hui Jin[a,b,*]

[a]School of Materials Science and Engineering, Shanghai Jiao Tong University, 800 Dongchuan Rd, Shanghai 200240, China
[b]National Engineering Research Center of Light Alloys and State Key Laboratory of Metal Matrix Composites, Shanghai Jiao Tong University, 800 Dongchuan Rd, Shanghai 200240, China

Received 12 March 2015; revised 30 April 2015; accepted 1 May 2015
Available online 28 May 2015

To reveal mechanical effects of intersecting shear flow in metallic nanoglass composites, thin film structured with layers of Al–Zr glass and columnar hexagonal grains of Cu–Zr glass has been studied with molecular dynamics. Pronounced homogeneous deformation beyond 10% of applied strain can be achieved at room temperature, either by impeding shear band formation through intergranular flow stagnation or by accommodating multiple shear banding flow through intragranular flow stagnation. Highly localized inhomogeneous flow or shear band can be suppressed effectively.

Keywords: Metallic glass; Nanoglass composite; Stagnation of viscous flow; Homogeneous/inhomogeneous deformation; Shear band

Metallic glass is a kind of noncrystalline or amorphous material normally obtained by quenching rapidly a liquid state into a solid state without crystallization. They may own a number of outstanding mechanical properties such as superior strength and exceptional hardness. Unfortunately, the lack of macroscopic plasticity or ductility at room temperature compromises their structural applications, typically due to unavoidable highly localized plasticity carriers called shear bands [1–3]. Up to now, only a few monolithic bulk metallic glasses (BMGs), e.g. Pt/Pd-rich metal–metalloid alloys [4,5] and Zr–Cu–Ni–Al alloy at properly selected compositions [6], have been found as exceptional cases. Comparing to other metallic glasses, when deformed they are featured by network of densely interlaced shear bands. The superior toughness seems relevant to nucleation and propagation of multiple shear bands.

To modify deformation behavior and thus to suppress catastrophic failure in metallic glasses, Gleiter proposed [7,8] that in analogy to nanocrystalline materials characterized by a high volume-fraction of crystal/crystal interfaces or grain boundaries (GBs), it might also be possible to introduce plenty of glass/glass interfaces (GGIs) into an "ordinary" glass and this new form of glass has been termed as "nanoglass" [9–14]. Because GGIs in nanoglass are regions of lower density or higher fraction of free-volume than that of grain glass, they are expected to flow easily so would be favorable to stabilize plastic deformation "homogeneously". A number of atomistic simulations [15–21], continuum modeling [22] and several experiments [23–25] in recent years have shown that the unique nanoglass microstructure is indeed capable to sustain high-density shear bands and consequently enhance the global plasticity. In particular, Wang et al. [25] have shown very recently that under uniaxial tension test, more than 15% plastic strain can be obtained for the $Sc_{75}Fe_{25}$ nanoglass, underlying that the evolution of multiple shear bands also plays essential roles.

However, what governs the flow properties of densely interweaved shear bands in either nanoglass or ordinary monolithic glass remains so far elusive. To examine how metallic glass accommodates intersecting shear flow and hence to understand the corresponding mechanical behavior, here we consider a nanoglass composite (NGC) as model material in our molecular dynamics (MD) simulations. Following Gleiter's nanoglass concept [7,8], a freestanding NGC thin film has been built by embedding 3 nm-thick $Al_{64}Zr_{36}$ glass layers into a block of $Cu_{64}Zr_{36}$ glass matrix, as shown in Figure 1a. The MD box representing the freestanding NGC film contains 1,083,156 atoms and is measured by 51.7 nm, 72.3 nm and 6 nm in x, y and z directions, respectively. Three-dimensional periodic boundary conditions (PBCs) are applied to the box (the supercell). The two free surfaces of the film are introduced in the x-direction of the supercell by including a vacuum region and the film thickness is 42 nm. Interatomic potentials for ternary Zr–Cu–Al alloys developed with embedded atom methods [26] have been employed throughout our MD simulations.

Binary glasses are obtained by heating the random solutions of corresponding alloys beyond 1250 K, relaxed for 2 ns to obtain liquids in thermal equilibrium, then quenched down to 10 K under a cooling rate of 10^{12} K/s, all at zero pressure conditions. Note that Cu–Zr binary

* Corresponding author at: School of Materials Science and Engineering, Shanghai Jiao Tong University, 800 Dongchuan Rd, Shanghai 200240, China.; e-mail: jinzh@sjtu.edu.cn

http://dx.doi.org/10.1016/j.scriptamat.2015.05.002
1359-6462/

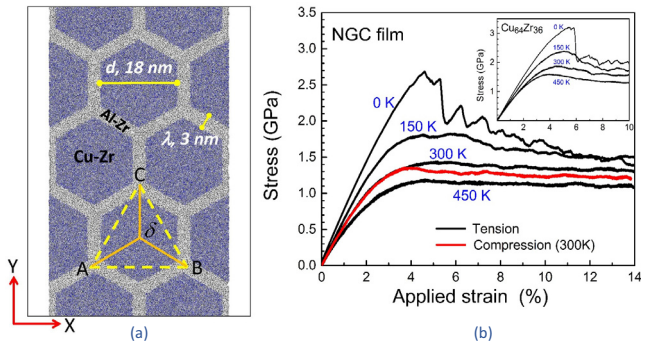

Figure 1. (a) Nanoglass composite (NGC) film. As marked schematically in a "flow path triangle" (*ABC*) chart, intersecting shear flow tends to meet at triple junction point or grain center (δ) but might also bypass the δ-point along the edge directions of the triangle. With grain size (d, 18 nm) and layer thickness (λ, 3 nm) as marked in the plot, the volume fraction (f) of soft layer is about 0.27 according to $f \approx 1 - d^2/(d+\lambda)^2$. Atoms are colored in blue for Cu, light gray for Al and dark gray for Zr. (b) Stress vs. applied strain curves obtained for NGC film and $Cu_{64}Zr_{36}$ film (inset). The calculated stress corresponds to the normal stress component (σ_{yy}) in the loading direction, i.e. the y-axis indicated in (a).

glasses have been well studied with MD simulations because the alloy systems exhibit good glass-forming ability in experiments [27,28]. The glass structures featured by pair distribution functions have been found to compare reasonably well with experimentally available data. According to calculated properties summarized in Table 1, the $Al_{64}Zr_{36}$ binary glass is taken to be the layer material because of its lower elastic moduli and higher Poisson ratio comparing to the $Cu_{64}Zr_{36}$ glass.

Uniaxial deformation is imposed on the film by applying homogeneous tensile or compressive strain (ε_{appl}) at a constant rate ($\dot{\varepsilon}_{appl} = 10^7\ s^{-1}$) in the y-direction, i.e. parallel to the set of potential flow path marked by "δC" in Figure 1a. In the z-direction of the supercell, the box length is kept constant. The deformation is carried out at three temperatures, i.e. 150 K, 300 K and 450 K, where the film system has been treated as canonical ensemble (*NVT*). Adiabatic deformation is also carried out with the system temperature set initially to be 0 K. For comparison, thin-film samples of monolithic $Cu_{64}Zr_{36}$ and $Al_{64}Zr_{36}$ binary glass have been simulated the same way. All calculations are carried out with *LAMMPS* package [29] with "OVITO" as visualization and auxiliary analysis tool [30].

The calculation of stress tensor is based on the standard linear response theory [31]. The microscopic *virial* stress in a deformed system is $\sigma_{\alpha\beta} = -\frac{1}{V}\sum_i \left[\frac{p_{i\alpha}p_{i\beta}}{m_i} + \sum_{j<i} r_{ij\alpha} f_{ij\beta}\right]$, $\alpha, \beta \in [1,3]$, where V measures the system volume, $p_{i\alpha}$ is the α-component of the momentum for the i-atom of a mass m_i, r_{ij} is the distance separating a pair of atoms i and j, and $f_{ij\beta}$ is the β-component of the force between the pair. From an initial MD configuration (the state at the moment t_0) to a final MD configuration (the state at the moment t), the non-affine atomic displacement for the i-atom is calculated via $\delta\mathbf{R}_i = \left(\mathbf{R}_i(t)H^{-1}(t) - \mathbf{R}_i(t_0)H^{-1}(t_0)\right)H(t)$, where H at t_0 or t is a 3×3 matrix representing the size and shape of the MD supercell, by which atomic displacement field (or velocity field of plastic flow) can be monitored. To examine more quantitatively the local plastic events, the *von Mises* atomic shear strain $\eta_i(t, t_0)$ is calculated from $\delta\mathbf{R}_i$ and H [32] where atoms within a cutoff radius of 4 Å are treated as neighbors.

When deformed adiabatically under tension, the film exhibits a sharp yield at $\varepsilon_{appl} \sim 4.53\%$, underlying a maximum stress (or yield strength) $\sigma_y \sim 2.64$ GPa (Fig. 1b). With increasing the ε_{appl} up to 15%, the tensile stress decreases to 1.3 GPa. The deformation is closely related to the formation and sliding of a 45° shear band, cutting-through Cu–Zr grain, leaving noticeable offset at free surfaces and solely capable to carry plastic flow, as illustrated by MD snapshot in Figure 2a–d. Vector field plots indicate that initial plastic events appear to follow somewhat "entangled" paths from one grain to another (Fig. 2a), not connectable with a straight line resembling a single shear band, underlying more than one set of shear bands tend to be initiated from opposite surface sites. Shear localization to a well-confined narrow band eventually occurs although it might be blocked temporarily, as indicated by stress jumping-up/down over the range $4.5\% < \varepsilon_{appl} < 7\%$ (Fig. 1b). Besides, shear-band sliding raises the system temperature to about 90 K as the applied strain approaches to 15%.

When tensile test is carried out at room temperature ($T = 300$ K), the stress–strain curve exhibits smooth yield behavior (Fig. 1b) with a moderate yield strength $\sigma_y \sim 1.43$ GPa at a larger applied strain ($\varepsilon_{appl} \sim 5.21\%$), followed by noticeable but weak softening. No shear banding flow occurs within the film up to 15% of applied strain. Instead, significant inward flow has been activated perpendicular to the loading direction as revealed by displacement field plot, Figure 2e–h. The horizontal plastic flow tends to impinge within Cu–Zr grains labeled as "1" and "2" in Figure 2b and f, such that the two grains have been squeezed up and exhibit an elongation of about 15%, although the applied tensile strain at this stage is 10%. In contrast, adjoining grains above and below (labeled as "3" and "4", respectively) have suffered much less deformation, i.e. merely 5% elongation in the loading direction. In other words, Cu–Zr grains "1" and "2" must deform faster than other grains as they impede much stronger inward plastic flow. Consequently, "necks" are produced at the

Table 1. Atomic volume (Ω), elastic moduli, shear modulus ($\mu = C_{44}$), Poisson ratio (ν), bulk modulus (B) and Young's moduli (E) calculated for Cu–Al–Zr glasses at 50 K.

MGs	Ω (Å^3)	C_{11} (GPa)	C_{12} (GPa)	C_{44} (GPa) or μ	ν	ν	B	E (GPa)
$Cu_{64}Zr_{36}$	16.16	144	99	22	0.409	0.409	114	62
				34[a]	0.352[a]	0.352[a]		92[a]
				21.6[b]	0.411[b]	0.411[b]		61[b]
$Cu_{32}Al_{32}Zr_{36}$	17.32	137	91.7	20.7	0.408	0.408	107	58.3
$Al_{64}Zr_{36}$	18.56	123.6	87.7	15.9	0.423	0.423	99.9	45.3

[a] Experimental data taken from [11].
[b] MD data taken from [10].